



# Gap junctional coupling between retinal amacrine and ganglion cells underlies coherent activity integral to global object perception

Kaushambi Roy<sup>a</sup>, Sandeep Kumar<sup>a</sup>, and Stewart A. Bloomfield<sup>a,1</sup>

<sup>a</sup>Department of Biological and Vision Sciences, State University of New York College of Optometry, New York, NY 10036

Edited by John E. Dowling, Harvard University, Cambridge, MA, and approved October 11, 2017 (received for review May 18, 2017)

**Cohesive spike activity occurs between widely separated retinal ganglion cells (RGCs) in response to a large, contiguous object, but not to disjointed objects. Since the large spatial separation between the RGCs precludes common excitatory inputs from bipolar cells, the mechanism underlying this long-range coherence remains unclear. Here, we show that electrical coupling between RGCs and polyaxonal amacrine cells in mouse retina forms the synaptic mechanism responsible for long-range coherent activity in the retina. Pharmacological blockade of gap junctions or genetic ablation of connexin 36 (Cx36) subunits eliminates the long-range correlated spiking between RGCs. Moreover, we find that blockade of gap junctions or ablation of Cx36 significantly reduces the ability of mice to discriminate large, global objects from small, disjointed stimuli. Our results indicate that synchronous activity of RGCs, derived from electrical coupling with amacrine cells, encodes information critical to global object perception.**

gap junctions | retina | perception | ganglion cells

**C**ohesive neuronal spiking, often in the form of oscillatory activity, is ubiquitous across the CNS, including all levels of the visual system (1–3). In the retina, neighboring retinal ganglion cells (RGCs) often show light-independent correlations with temporal precision ranging from synchronous activity to relatively loose cross-correlation profiles spanning tens of milliseconds (4–9). The RGCs also display coherent activity strongly dependent on light stimulus parameters, including intensity, size, contrast, and movement (10–12). However, the role of coherent activity in the visual system remains unclear. Studies show that concerted spiking of RGC neighbors provides additional information to the brain, up to 20% more in the primate, which is multiplexed with asynchronous activity from individual RGCs, thus overcoming the limited bandwidth of the optic nerve (13, 14). Conversely, spike correlations could be disadvantageous in some cases, in which, reflecting inefficient redundancy of signals inherent to massive interconnectivity of cells, they actually limit coding of information (15–18).

It has been posited that light-dependent correlated activity of visual neurons serves to segregate distributed features in an image, thereby defining stimulus structure important for binding and perceptual discrimination of local and global objects (19–21). In classic experiments, Neuenschwander and Singer (10) showed that correlated spike activity of RGCs in the cat retina could occur over surprisingly long distances, up to 20° of visual angle, provided that the large stimuli used to activate cells are contiguous. These long-range RGC correlations were reliably transmitted to geniculate neurons and appeared to contribute, at least in part, to synchronizations at the cortical level (10). It was thus posited that long-range coherence of RGC activity encodes visual information pertinent to perceptual grouping and thereby plays a critical role in global object recognition.

How these long-range correlations occur between distant RGCs is unclear as their sizeable separation eliminates shared excitatory inputs from a common cohort of bipolar cells. Electrical coupling via gap junctions (GJs) is believed central to the

cohesive spike activity of neuronal ensembles in the CNS, including the retina (22–24). Interestingly, many RGCs are coupled indirectly via GJs made with amacrine cells (ACs), most of which fall into the polyaxonal (PAC) subtype category based on their extensive processes that can span >1 mm (25–27). Such far-reaching RGC–AC electrical coupling forms excitatory circuits that can plausibly support the correlated activity between widely separated RGCs.

Here, we tested this idea by examining correlated activity between distant RGCs in the mouse retina with different gap junctional coupling patterns to small separate and large contiguous light stimuli. Our results show that large contiguous stimuli evoke a significant increase of coherent activity between distant RGCs that are coupled indirectly over long distances via PACs. Moreover, pharmacological blockade of these GJs or genetic ablation of their subunit connexins, specifically connexin36 (Cx36), abolishes the coherent activity evoked by large contiguous objects. Furthermore, GJ blockade or connexin ablation significantly reduces the ability of mice to discriminate large contiguous objects from smaller disjointed ones. Our findings thus indicate that electrical coupling between RGCs and PACs underlies long-range coherent activity in the retina, which provides information to the brain critical to global object perception.

## Results

**Paired RGC Recording Paradigm in the Kcng4-cre;Thy1-stop-YFP Line 1 Mouse.** In initial experiments, our study focused on the ON α-RGCs in the mouse retina, which are coupled indirectly via

### Significance

**Neuron ensembles in the brain visual system often show correlated responses, but the sensory information encoded by this activity remains unclear. Here, we show that widely separated ganglion cells in the mouse retina show correlated activity when presented with a large, contiguous object, but not when the object is disjointed. We show that these long-range correlations are produced by electrical coupling via gap junctions made with polyaxonal amacrine cells, which can span distances greater than a millimeter. Blockade or ablation of these gap junctions eliminates correlations between distant ganglion cells and, moreover, diminishes an animal's ability to discriminate large, solid objects from disjointed ones. Our findings indicate that long-range correlated activity in the retina encodes visual information critical for global object perception.**

Author contributions: K.R. and S.A.B. designed research; K.R., S.K., and S.A.B. performed research; K.R., S.K., and S.A.B. analyzed data; and K.R., S.K., and S.A.B. wrote the paper. The authors declare no conflict of interest.

This article is a PNAS Direct Submission.

Published under the PNAS license.

<sup>1</sup>To whom correspondence should be addressed. Email: sbloomfield@sunyopt.edu.

This article contains supporting information online at [www.pnas.org/lookup/suppl/doi:10.1073/pnas.1708261114/-DCSupplemental](http://www.pnas.org/lookup/suppl/doi:10.1073/pnas.1708261114/-DCSupplemental).

GJs made with two or more subtypes of PACs (25–27). We used the Kcng4-cre;Thy1-stop-YFP line 1 (Kcng4-YFP) mouse line in which the ON and OFF  $\alpha$ -RGC subtypes uniquely express yellow fluorescent protein (YFP) in the ganglion cell layer (GCL) and thereby can be visualized and targeted for electrophysiological recordings (28, 29) (Fig. 1A). Immunolabeling for SMI32, a marker for  $\alpha$ -RGC cell bodies and axons (29, 30), confirmed the identity of the YFP-expressing cells in the GCL of Kcng4-YFP mice as the  $\alpha$ -subtype (Fig. 1A). We initially targeted pairs of sustained ON  $\alpha$ -RGCs with nonoverlapping receptive field centers for loose patch recordings (Fig. 1B–D). Cell somata that were typically separated by ~300–600  $\mu$ m, corresponding to 12–24° of visual angle, were visualized and recorded. We stimulated cell pairs with either two discreet rectangles of light placed over each cell soma or a large, single rectangular bar of light that extended over and covered both receptive field centers, thus representing local vs. global objects, respectively. To determine the coherent spike activity of cell pairs, we generated cross-correlogram profiles (CCPs) for the light-evoked responses, which revealed correlated activity exceeding chance as histogram peaks above the 99% confidence level (red line; Fig. 1E). To demonstrate spike correlations between  $\alpha$ -RGC pairs that were not time-locked to the light stimulus, data were time shuffled using a shift-predictor protocol, which was then subtracted from the original CCP (31) (Fig. 1F).

**Long-Range Coherent RGC Activity Is Dependent on GJ Coupling.** Widely separated ON  $\alpha$ -RGC pairs were first stimulated independently with small rectangular lights centered over their YFP-expressing somata to map their receptive field centers and to confirm that they were nonoverlapping. Cells were injected with Neurobiotin (NB) to determine their dendritic field morphology and tracer coupling with PACs, by post hoc histology, to confirm their  $\alpha$ -cell identity (Fig. 2A). The rectangles of light were then presented simultaneously, evoking light-evoked ac-

tivity as indicated in PSTHs ( $n = 7$  pairs of cells; Fig. 2B). The shift predictor CCPs generated from the responses of ON  $\alpha$ -RGC pairs to the separate rectangles of light showed no coherent activity (Fig. 2C). In contrast, we observed a dramatic increase in coherent activity when the two rectangles were merged into a single contiguous rectangle that spanned the receptive fields of ON  $\alpha$ -RGC pairs, (Fig. 2D and E), confirming findings in cat retina (10). The shift predictor CCP profile showed a single peak at 0 s, indicating a prominent spike synchrony with a bandwidth of approximately  $\pm 10$  ms. Interestingly, this type of CCP profile is believed to reflect indirect electrical coupling of RGCs via intermediary ACs, consistent with the coupling pattern of ON  $\alpha$ -RGCs (8, 32). We did find that presentation of the contiguous rectangle increased the level of spike activity of  $\alpha$ -RGCs compared with that evoked by smaller, disjointed stimuli. However, a comparison of spike activity of the pairwise recordings made throughout this revealed no relationship between the level of RGC spike activity and the degree of coherent firing.

We presented a number of different stimulus shapes and contours and evaluated how these affected long-range synchronous activity between RGC pairs. Presentation of discontinuous rectangles divided into three segments also did not produce coherent activity between ON  $\alpha$ -RGC pairs ( $n = 3$  pairs of cells; Fig. S1A). In contrast, presentation of large stimuli of various shapes and sizes invariably produced long-range correlated activity between distant ON  $\alpha$ -RGC pairs, provided that they covered the receptive field centers of the individual cells and spanned the intermediate regions contiguously ( $n = 3$  pairs of cells; Fig. S1 B–F).

To determine whether electrical coupling was critical to long-range coherent activity between ON  $\alpha$ -RGC pairs, retinas were superfused with the nonselective GJ blocker meclofenamic acid (MFA) before the presentation of disjointed and contiguous light stimuli. Although the light-evoked responses were preserved

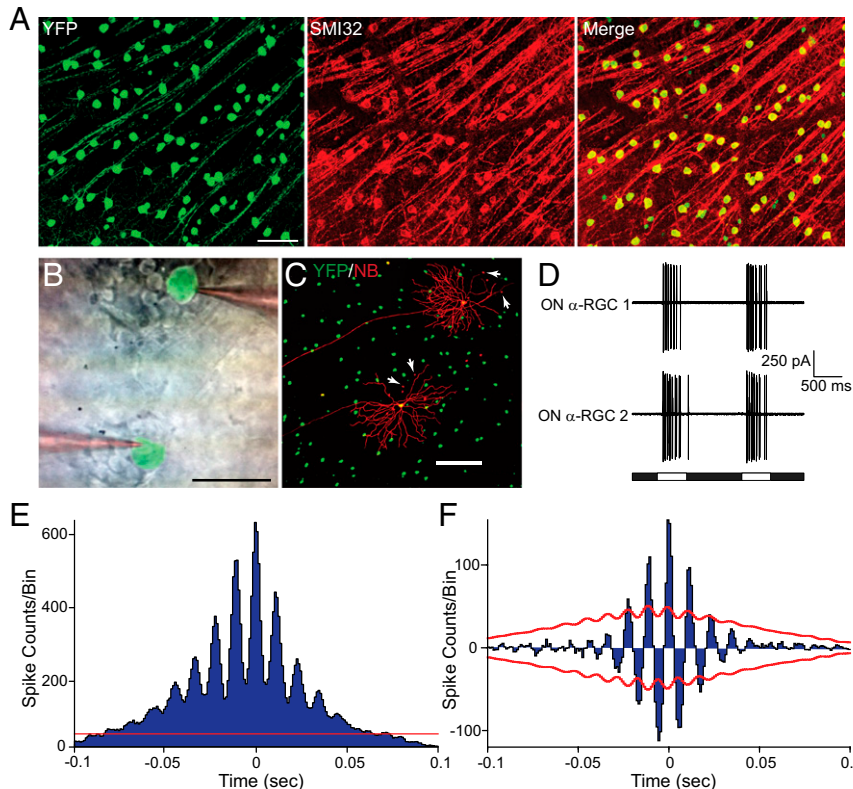


**Fig. 1.** Pairs of YFP-expressing  $\alpha$ -RGCs in the Kcng4-YFP mouse retina were visualized and targeted for electrophysiological recording. (A) The Thy1-positive Kcng4-YFP mouse retina displays YFP-expressing  $\alpha$ -RGCs. The retina was immunolabeled for SMI32 antibody, and the merged image shows that >90% of YFP<sup>+</sup> cells in the GCL colocalized with SMI32 labeling, confirming their  $\alpha$ -subtype identity. (Scale bar, 100  $\mu$ m.) (B) Example of the recording paradigm showing dual loose-patch electrodes recording a pair of  $\alpha$ -RGCs in the Kcng4-YFP mouse retina. Note that, for illustrative purposes, the distance between the cells in the panel is smaller than that of cell pairs from which actual data were collected. (Scale bar, 50  $\mu$ m.) (C) YFP-expressing ON  $\alpha$ -RGCs in Kcng4-YFP mouse retina filled with Neurobiotin (NB) exemplifies the separation of cell pairs from which recordings were made. Arrows indicate tracer-coupled AC somata. (Scale bar, 200  $\mu$ m.) (D) Loose patch recordings from a pair of ON  $\alpha$ -RGCs show spike responses to separate rectangular stimuli placed over each cell body. Stimuli onset and offset are indicated by traces at Bottom of the panel. (E) Example of a raw CCP computed from light-evoked spikes recorded from a pair of ON  $\alpha$ -RGCs. Red line represents the 99% confidence above which correlations are above chance. (F) Same CCP as in E after subtraction of the time shuffling using a shift predictor paradigm.

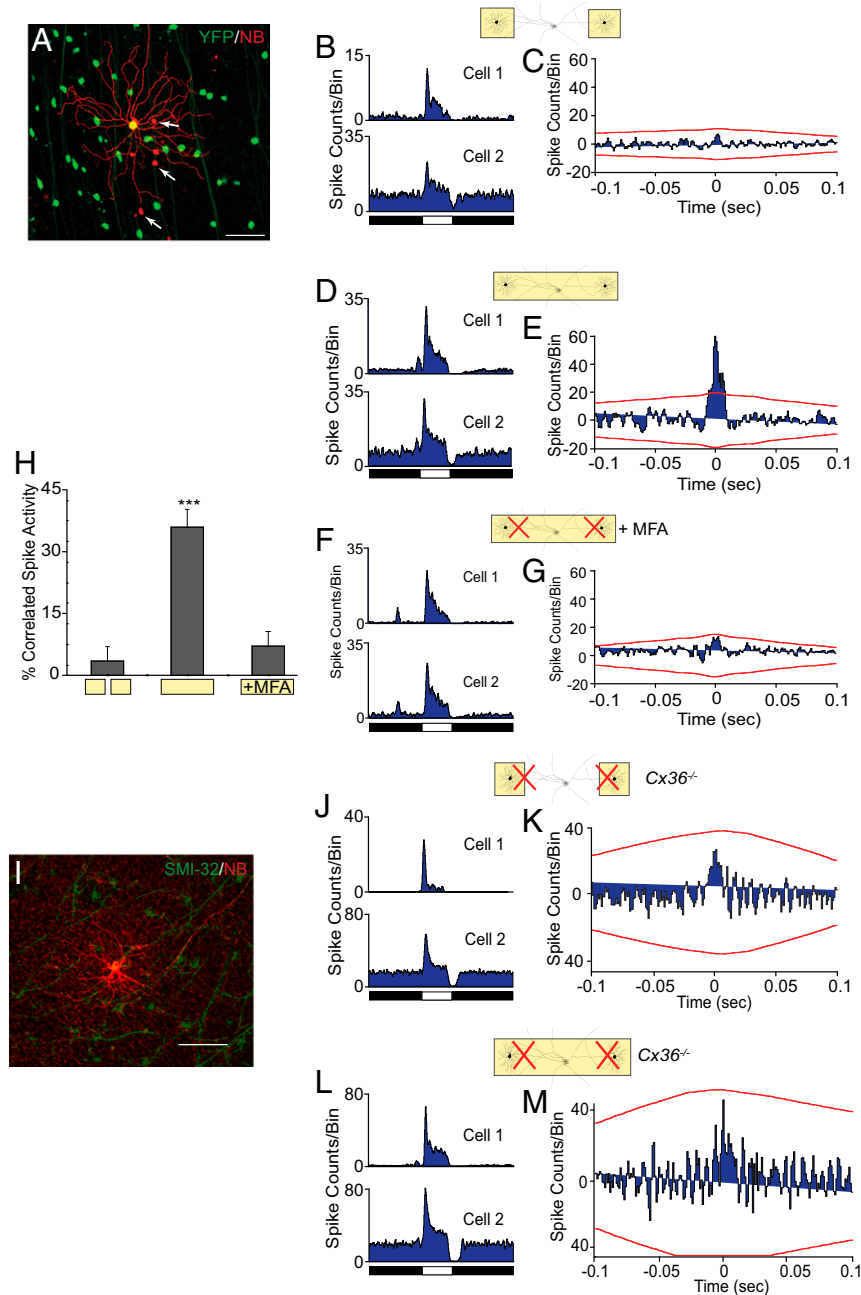


**Fig. 2.** Long-range correlated activity of ON α-RGC pairs in response to a large, contiguous stimulus is abolished by pharmacological blockade or genetic ablation of GJs. (A) An ON α-RGC in the Kcng4-YFP mouse retina shows tracer coupling to ACs (arrows). (Scale bar, 100 μm.) (B) Peristimulus time histograms (PSTHs) generated from a pair of ON α-RGCs in the Kcng4-YFP mouse retina in response to 0.5-s duration presentation of two rectangular light stimuli restricted to the receptive field center of each cell (Inset). (C) Shift predictor CCP generated from the same pair of ON α-RGCs in B in response to two discreet rectangular light stimuli shows no coherent activity. (D) PSTHs from the same pair of ON α-RGCs as in B in response to presentation of a contiguous rectangular light stimulus formed by fusing the separate rectangles (Inset). (E) Shift predictor CCP generated from the same pair of ON α-RGCs as in C in response to the contiguous rectangular stimuli. CCP shows clear synchronous activity between the cell pair. (F) PSTHs from the same pair of ON α-RGCs in response to presentation of the contiguous light stimulus after the application of MFA. (G) CCP generated from recordings made from the same pair of ON α-RGCs as in E after the application of MFA to block GJs shows that synchronous activity is abolished. (H) Cumulative histogram from seven pairs of ON α-RGCs shows that correlated activity is evoked by a contiguous light stimulus, which is abolished by application of the GJ blocker MFA. One-way ANOVA followed by Tukey's multiple-comparison test;  $\alpha = 0.05$ ; \*\*\* $P < 0.001$ ; data presented as mean  $\pm$  SEM. (I) Single ON α-cell filled with NB in the Cx36<sup>-/-</sup> mouse retina shows loss of coupling to ACs. Retina was immunolabeled with SMI-32 to confirm that the labeled cell is a α-RGC. (Scale bar, 100 μm.) (J) PSTHs generated from the light-evoked activity of a pair of ON α-RGC in a Cx36<sup>-/-</sup> mouse retina in response to a 0.5-s presentation of two separate rectangles restricted to the receptive field center of each cell (Inset). (K) CCP computed from the same pair of ON α-RGC in J shows no correlated activity in response to separate rectangles. (L) PSTHs from the same pair of ON α-RGC in J in response to a contiguous rectangular stimulus formed by fusing the separate rectangles. (M) CCP computed from the same pair of cells in K shows no increase in coherent activity in response to a single large rectangle.

(Fig. 2F), application of MFA completely abolished the synchronous activity, indicating that gap junctional coupling was necessary for coherent spiking between distant RGC pairs (Fig. 2 G and H).

We also recorded from pairs of ON α-RGCs in C57BL/6 and CxWT mouse strains by targeting cells in the GCL with large somata and confirming their identities with NB labeling and post

hoc histology (Fig. S2 A and E). Similar to the findings in Kcng4-YFP mice, pairs of distant ON α-RGCs in both C57BL/6 and *CxWT* animals showed no coherent activity in response to separate rectangles of light, but displayed significant spike syn-

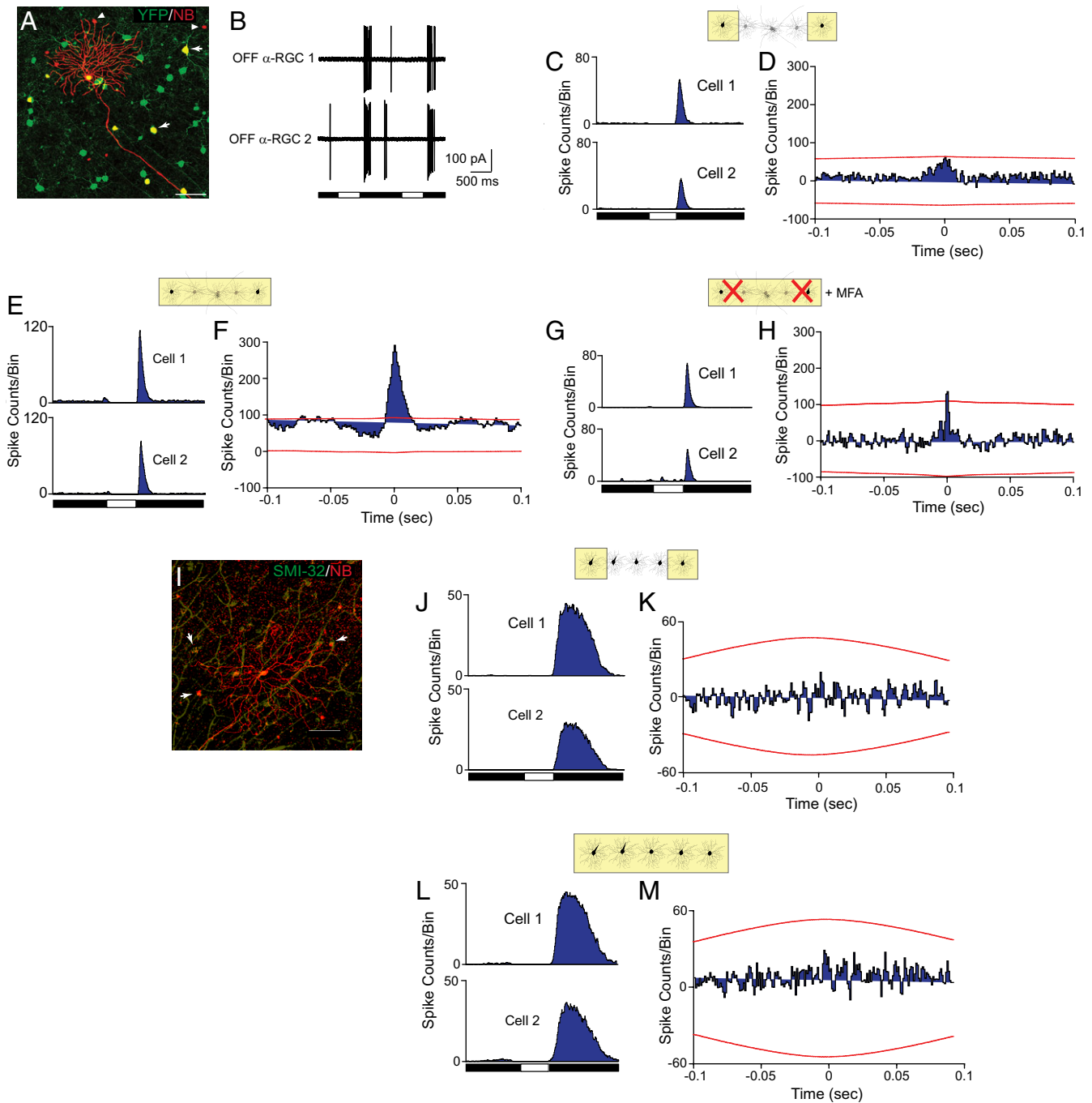


**Fig. 3.** Serial direct coupling between RGCs does not evoke long-range correlated spike activity between OFF α-RGCs. (A) Micrograph of an OFF α-RGC filled with NB in the Kcng4-YFP mouse retina shows coupling to both ACs (arrowheads) and neighboring OFF α-RGCs (arrows). (Scale bar, 100 μm.) (B) Responses of a pair of OFF α-RGCs to separate rectangles of light restricted to the receptive field of each cell. (C) PSTHs generated from the light-evoked activity of a pair of OFF α-RGCs in a Kcng4-YFP mouse retina in response to presentation of two discrete 0.5-s duration rectangular light stimuli (Inset). (D) Shift predictor CCP computed from the pairs of OFF α-RGCs in response to separate rectangles shows no coherent firing. (E) PSTHs from the same OFF α-RGC pair as in C in response to 0.5-s presentation of a contiguous rectangle (Inset). (F) CCP from the same pair of OFF α-RGCs in D in response to the contiguous rectangle shows a significant increase in correlated activity. (G) PSTHs from the pair of OFF α-RGCs in C in response to the contiguous rectangular light stimulus after the application of MFA. (H) CCP shows that application of MFA largely abolished the long-range synchronous activity between the same pair of OFF α-RGCs as in F in response to a contiguous rectangular stimulus. (I) An OFF α-RGC in the *Cx36<sup>-/-</sup>* mouse retina filled with NB shows loss of coupling to ACs, but homologous coupling between OFF α-RGCs (arrows) is preserved. (Scale bar, 100 μm.) (J) PSTHs from a pair of OFF α-RGC in a *Cx36<sup>-/-</sup>* mouse retina in response to 0.5-s presentation of two rectangular light stimuli (Inset). (K) CCP computed for the pair of OFF α-RGC in J in response to two separate light stimuli shows no coherent activity. (L) PSTH generated from the same pair of OFF α-RGCs in J in response to a fused, contiguous single rectangle. (M) CCP computed for the same pair of OFF α-RGCs in K still shows no correlated activity when the separate rectangles of light were fused into a single object.

chrony when the rectangular stimuli were fused into a single contiguous object ( $n = 3$  pairs of cells for each strain; Fig. S2 B, C, F, and G). Furthermore, blockade of GJs with MFA effectively abolished the long-range correlations between ON  $\alpha$ -RGCs in both wild-type mouse strains ( $n = 3$  pairs of cells for each strain; Fig. S2 D and H). In separate experiments, we found that application of another nonselective GJ blocker, 18 $\beta$ -GA, also abolished all long-range synchronous activity between ON  $\alpha$ -RGCs in the Keng4-YFP mouse retina when evoked with a large, contiguous stimulus ( $n = 3$  cell pairs; Fig. S3).

Previous studies have shown that the GJs coupling ON  $\alpha$ -RGCs to PACS contain Cx36 subunits (26, 32–34). We therefore tested whether genetic ablation of Cx36 in the Cx36<sup>−/−</sup> mouse strain disrupted long-range coherent spiking between ON  $\alpha$ -RGCs. Injection of NB into single ON  $\alpha$ -RGCs retinas failed to label ACs, confirming that the interconnecting GJs were ablated in the Cx36<sup>−/−</sup> mouse (Fig. 2I). Presentation of separate rectangles of light covering the receptive field centers of widely separated ON  $\alpha$ -RGC pairs or a fused, contiguous rectangle both evoked robust spike activity (Fig. 2 J and L), but neither produced significant coherent firing ( $n = 5$  pairs of cells; Fig. 2 K and M). Taken together, these data support the idea that functional GJs between RGCs and PACs are essential for generation of synchronous activity between distant ON  $\alpha$ -RGCs in response to global object presentation.

**Serial Direct Coupling Between RGCs Does Not Support Long-Range Coherent Activity.** Next, we extended experiments to pairs of distant OFF  $\alpha$ -RGCs in the Keng4-YFP mouse retina, which, like ON  $\alpha$ -RGCs, are coupled to PACs but are also coupled homologously to one another (26, 33, 34) (Fig. 3A). Presentation of separate rectangular stimuli centered over the somata of widely separated (300–600  $\mu$ m) OFF  $\alpha$ -RGCs evoked robust transient or sustained activity at stimulus offset (Fig. 3 B and C) but failed to evoke coherent activity as assayed by the shift predictor CCPs ( $n = 3$  cell pairs; Fig. 3D). In contrast, when the rectangles of light were extended and fused into a single stimulus, the OFF  $\alpha$ -RGCs showed significant synchronous activity (Fig. 3 E and F), similar to that shown for ON  $\alpha$ -RGC pairs. Although the light-evoked activity of the RGCs was preserved following blockade of GJs with MFA (Fig. 3G), the spike coherence was largely abolished, although a small residual synchrony was often detected near the 99th percentile significance level in the CCPs (Fig. 3H). This suggested that some residual coupling, possibly the direct coupling between OFF  $\alpha$ -RGCs may have contributed to the long-range coherent activity. We therefore examined whether direct RGC-RGC coupling was sufficient to produce long-range spike synchrony. Earlier studies reported that OFF  $\alpha$ -RGCs in the Cx36<sup>−/−</sup> mouse show only direct homologous coupling, as GJs made with ACs are ablated (33, 34). We therefore targeted pairs of RGCs with large somata in Cx36<sup>−/−</sup> mice that showed OFF-center receptive field physiology. Cells were injected with NB for post hoc histological identification, and retinas were immunolabeled for SMI32 to confirm that cell pairs were OFF  $\alpha$ -RGCs (Fig. 3I). Recordings from pairs of distant OFF  $\alpha$ -RGCs showed that presentation of separate, rectangular stimuli to their individual receptive field centers evoked rather sustained responses at stimulus offset (Fig. 3J), but produced no coherent activity ( $n = 4$  cell pairs; Fig. 3K), similar to that found for ON and OFF  $\alpha$ -RGCs in control Keng4-YFP and CxWT mice (Figs. 2C and 3D and Fig. S2F). However, in contrast to findings in control animals, presentation of a large, contiguous rectangle failed to produce synchronous activity between OFF  $\alpha$ -RGC pairs in Cx36<sup>−/−</sup> mice (Fig. 3 L and M). Thus, direct serial coupling between OFF  $\alpha$ -RGCs was insufficient to produce long-range coherent activity.

**Pairs of Different RGC Subtypes, Which Are Not Coupled, Do Not Show Long-Range Coherent Activity.** To further examine whether gap junctional coupling is necessary for long-range coherent activity between RGCs, we extended experiments to RGC pairs formed by different subtypes. Previous studies suggest that different subtypes of RGCs do not form GJs with one another or to a common cohort of ACs (26, 27). In these experiments, recordings were made from a YFP-expressing  $\alpha$ -RGC in the Keng4-YFP retina and a second RGC (cells with somata >15  $\mu$ m in diameter were targeted to avoid displaced ACs) with the same ON/OFF receptive field polarity, but devoid of YFP expression, indicating a different subtype identity. Separate rectangles of light were presented over the individual somata to evoke robust responses and to confirm that the cells had nonoverlapping receptive field centers (Fig. 4A). Recordings made from dissimilar pairs of RGCs did not show coherent activity to either separate or fused rectangular stimuli ( $n = 5$  cell pairs; Fig. 4 B–D).

**Incremental Fusing of Separate Stimuli Reveals a Threshold Property of the Long-Range Coherent Activity Between RGCs.** Our results clearly showed that, while presentation of separate stimuli covering the respective receptive field centers of distant RGCs did not produce coherent activity, merging of the stimuli into a single global object induced significant long-range spike synchrony. We next examined the process by which spike synchrony emerged between ON  $\alpha$ -RGC pairs as the separate rectangular stimuli were incrementally fused. For these experiments, the two rectangular stimuli were first centered over the somata of the distant ON  $\alpha$ -RGCs and were subsequently elongated symmetrically and incrementally to fusion ( $n = 6$  cell pairs; Fig. 5 A–J). Interestingly, we found that long-range synchronous activity did not emerge in a linear fashion related to stimulus separation, but rather showed a clear threshold characteristic. Stimuli could be separated by as little as 20  $\mu$ m (the smallest separation possible using our stimulus software) without evoking a significant increase in spike synchrony between pairs of ON  $\alpha$ -RGCs. In contrast, fusion of the rectangles into a single, large contiguous object spanning the receptive field centers of cell pairs produce a dramatic increase in synchronous activity (Fig. 5K).

**Stimulus Presentation to the Intermediary Zone Between Distant RGCs Does Not Evoke Long-Range Coherent Activity.** Our results suggested that activity of PACs coupled to RGCs produces the long-range coherent spiking to global stimuli. Therefore, in the next series of experiments, we examined whether stimulation of these ACs alone with a small, solid stimulus could also evoke the same long-range coherent activity as produced by a global stimulus. Although coupled homologously to each other, individual PACs show relatively small center receptive fields, suggesting that inputs are restricted to the most proximal processes (25, 35, 36). We therefore presented a single rectangle to the intermediary zone between and outside the receptive fields of a pair of widely separated ON  $\alpha$ -RGCs, with the presumption that this configuration would directly stimulate PACS and not the RGCs to which they were coupled. Interestingly, light presentation to the intermediary zone between two distant ON  $\alpha$ -RGCs produced only weak light-evoked responses and failed to produce correlated activity ( $n = 6$  cell pairs; Fig. 6 A–D). Robust light-evoked activity and coherent activity were not observed until the light stimulus was extended to cover, at least in part, the receptive field centers of the ON  $\alpha$ -RGCs (Fig. 6 E–J). An analysis of the correlated spikes indicated that a significant increase in long-range coherence was evoked only when the rectangular stimulus covered at least one-half of the dendritic arbor of each of the  $\alpha$ -RGCs (Fig. 6K). These results suggest that stimulation of PACs alone was ineffective in producing long-range correlated spiking between RGCs. Similar results were found using stimuli with an ovoid configuration (Fig. S1 D–F).

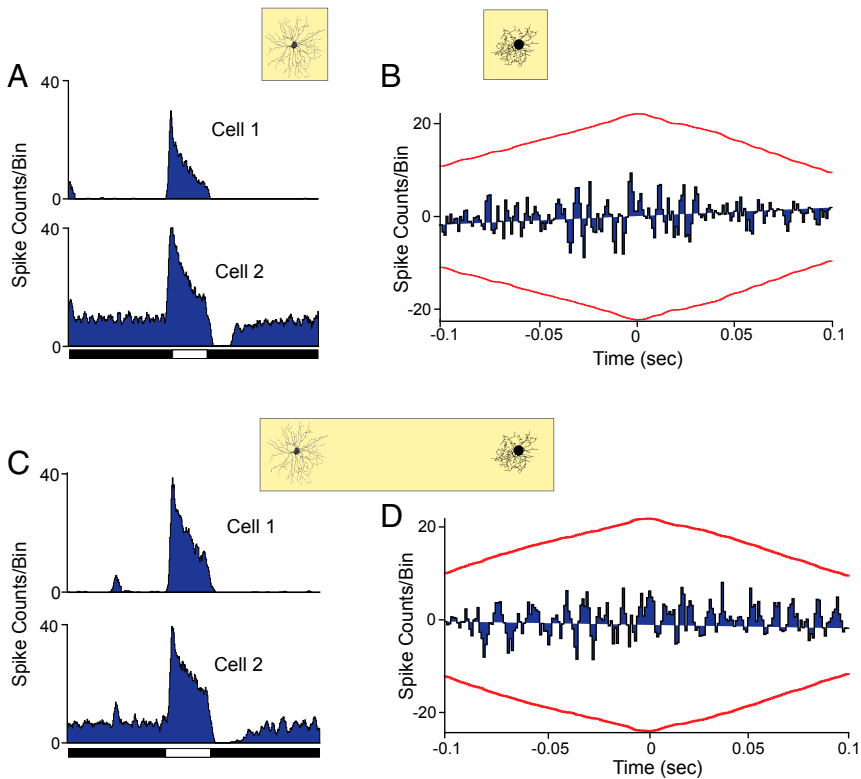


**Fig. 4.** Uncoupled RGCs show no long-range correlated firing in response to a contiguous light stimulus. (A) PSTHs generated from the responses of an ON  $\alpha$ -RGCs in the Kcng4-YFP mouse retina and a distant ON RGC that did not express YFP and was therefore of another subtype in response to two 0.5-s duration rectangular light stimuli placed over their respective receptive field centers (Inset). (B) CCP computed from the same pair of cells in A showed no coherent activity in response to simultaneous presentation of the two rectangles of light. (C) PSTHs from the same pair of RGCs as in A in response to a fused, contiguous rectangle. (D) CCP generated from the same pair of RGCs as in B in response to a fused rectangle showed no coherent spike activity.

**GJ Blockade Reduces Global Object Perception in Mice.** It has been proposed that long-range coherent activity between distant RGCs underlies global object perception (10). We therefore examined whether pharmacological blockade of GJs or deletion of Cx36, both of which we found eliminated long-range synchronous activity between distant RGCs, attenuated an animal's ability to discriminate a contiguous global object from smaller discontinuous stimuli. In initial experiments, we trained *CxWT* mice on a Y water maze global task to discriminate a solid rectangle from one in which the rectangle was divided into two parts separated by 1–20° of visual angle ( $n = 5$  animals; Fig. 7G). We then made bilateral intraocular injections of MFA into the mice and retested them. In control experiments, we found that intraocular injections with MFA uncoupled RGCs from ACs cells for up to 7 d ( $n = 3$  eyes; Fig. 7A–F). Sham injections of 0.1 M PBS indicated that animals' performance on the discrimination task and visual acuity test at 48 h after injection was unchanged from preinjection levels ( $n = 3$ ;  $P > 0.1$ ). Therefore, animals were retested beginning 48 h and within 1 wk after the MFA injections. In complementary experiments, we trained *Cx36<sup>−/−</sup>* mice ( $n = 5$  animals) on the Y maze test and then compared their discrimination ability to that of *CxWT* littermates. We found that *CxWT* control animals could readily discriminate contiguous rectangles from two rectangles that were separated by as little as 2° of visual angle, but failed the discrimination test when the separation was reduced to 1.5° or 1.0° (Fig. 7H). However, both MFA-injected *CxWT* mice and *Cx36<sup>−/−</sup>* mice did significantly worse than control mice on the Y water maze task as they were unable to reliably discriminate a contiguous rectangle from two rectangles separated by 7° or less (Fig. 7H). In a final set of experiments, we examined whether the

reduced discrimination ability of the MFA-injected *CxWT* ( $n = 5$  animals) and *Cx36<sup>−/−</sup>* mice ( $n = 5$  animals) compared with control animals may have reflected a general attenuation in spatial acuity. Animals were therefore trained on the Y water maze to discriminate sinusoidal gratings with different spatial frequencies from a solid gray stimulus (37). We found no difference between *CxWT*, MFA-injected *CxWT*, or *Cx36<sup>−/−</sup>* mice in their ability to discriminate spatial frequencies of 0.1–0.5 cycles/degree (cpd), which corresponded to the normal spatial acuity of C57BL/6 mice (37) (Fig. 7I).

## Discussion

The present results provide strong evidence that electrical synaptic circuitry in the retina, specifically mediated by Cx36 containing GJs, is responsible for generation of the long-range coherent spiking between distant RGCs evoked by large, contiguous light stimuli. Since Cx36-expressing GJs exist at all levels of the retina and MFA is a nonspecific blocker, these data do not reveal conclusively which GJ cohorts subserve the long-range coherent firing. Nevertheless, with these caveats in mind, the results strongly suggest that the GJs that couple  $\alpha$ -RGCs and PACs (33, 34) form the portals by which excitation from intermediary ACs can synchronize activity between distant RGCs to which they couple. First, it has been shown that  $\alpha$ -RGC–PAC coupling is abolished in the *Cx36<sup>−/−</sup>* mouse retina, indicating that the GJs that link them contain Cx36 (33, 34). Second, the PACs uniquely form ideal mediators of long-range interactions: their receptive fields are relatively small, indicating inputs limited to proximal processes, but they display sodium-mediated axonal spikes that can propagate signals along the different axonal segments centrifugally over millimeters to distant targets (25, 35,

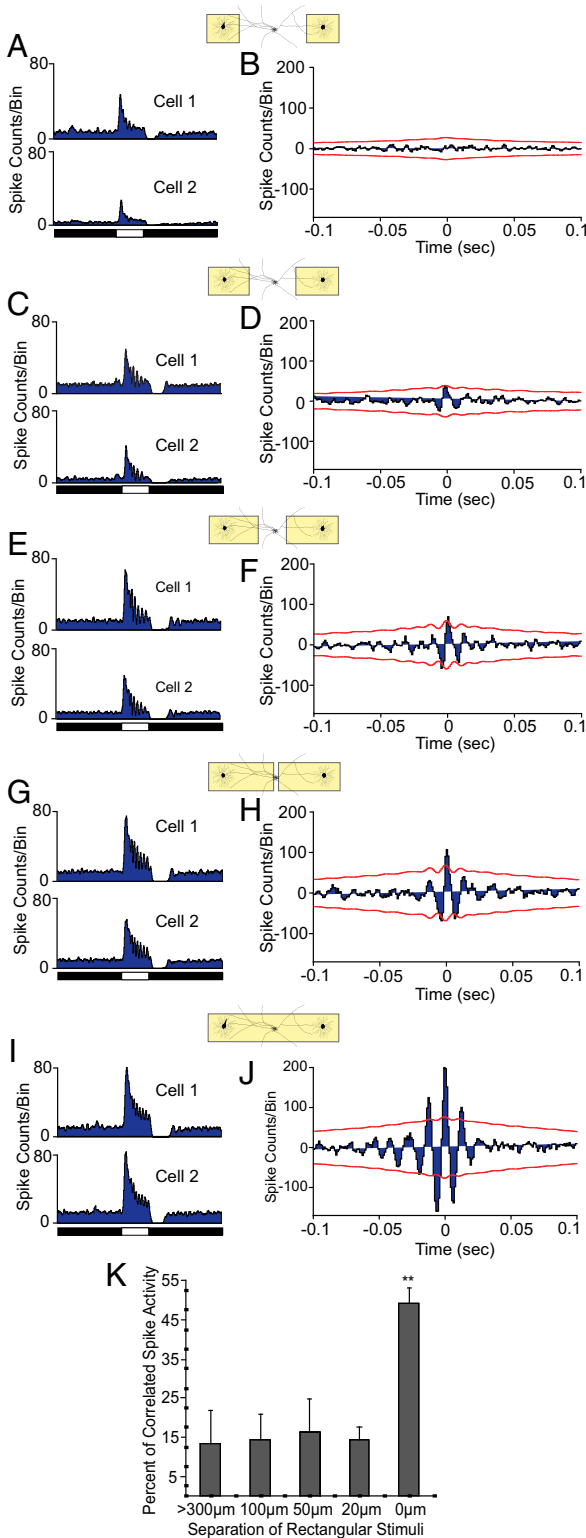


**Fig. 5.** Incremental fusing of separate light stimuli reveals a threshold characteristic of coherent activity between RGC pairs in terms of stimuli separation. (A–J) PSTHs (A, C, E, G, and I) and the corresponding shift predictor CCPs (B, D, F, H, and J) were computed from the light-evoked activity of a pair of ON α-RGC in the Kcng4-YFP mouse retina in response to two separate rectangular light stimuli presented for 0.5 s that were incrementally fused in discrete steps (A and B, >300 μm; C and D, 100 μm; E and F, 50 μm; G and H, 20 μm; I and J, 0 μm). The CCPs showed that significant correlated activity occurred only when the stimuli were completely fused. This demonstrates that coherent activity has a threshold in terms of stimuli separation.

36). No other neuronal type in the retina has the spatial extent to subserve the long-range coherence, except through serial coupling. However, we found that serial coupling, at least for RGCs, was incapable of supporting long-range coherent activity. We therefore posit that the spikes propagating along the different axonal segments to the widely separated RGCs are temporally correlated as they are derived from somatic spike activity (25). In turn, the axonal spikes drive coherent spike activity in the electrically coupled RGCs. Gap junctional coupling to ACs with enormous arbors has been reported for many different RGC subtypes across a number of species (25, 26, 34, 36, 38, 39). Therefore, whereas we restricted our study to α-RGCs because they could be easily visualized and targeted in the Kcng4-YFP mouse, it is likely that many other RGC subtypes also show long-range interactions via electrical coupling with ACs. Interestingly, long-range synaptic inhibition mediated by PACs, which are GABAergic (40–43), is believed to play a role in peripheral or shift effects that extend beyond the classic center/surround receptive fields of RGCs (44–46). Thus, PACs may play dual, opposing roles with chemical synaptic output providing inhibition and electrical synapses delivering direct excitation to distant RGCs. In contrast, a computational modeling study suggested that both the inhibition and excitation provided by PACs play a complementary role in synchronizing the oscillatory activity of RGCs (47). While our results support the idea that excitatory outputs from PACs via GJs are critical for long-range synchrony of distant RGC activity, whether inhibitory outputs have a role is currently unclear.

Whereas electrical coupling between RGCs and PACs can support long-range coherent spiking, our results indicate that serial coupling between RGCs cannot sustain this activity. These data are consistent with tracer coupling studies, which showed that NB injected into single RGCs will diffuse only across first-tier GJs and thereby label only nearest-neighbor RGCs (12, 26, 27, 48). The limited tracer movement is thought to reflect the relatively low conductance of certain RGC GJs in the inner retina, which limits the lateral spread of visual signals that would otherwise result in unwanted blurring of the image. Direct RGC–RGC coupling may thereby play roles in the encoding and integration of local image features.

Experiments in which the separation between the two rectangular stimuli was incrementally changed showed that the long-range synchronous activity between ON α-RGCs did not increase proportionally, but rather showed a threshold characteristic. These data are consistent with a computational model of PAC innervation of RGCs, which predicted that synchronous activity would fall off sharply as a solid object spanning an RGC pair receptive fields was separated (49). The sudden loss of RGC coherent activity when a solid rectangle was separated suggests induction of a suppressive mechanism, which was incorporated into the computer model (49). A GABAergic inhibition has previously been shown to effectively shunt intercellular currents propagating through GJs that couple ACs and ON direction-selective RGCs (50). In this regard, it is interesting to note that presentation of stimuli to an intermediary zone between RGC pairs did not evoke long-range coherence, but synchronous activity emerged only when the stimulus was extended to cover the receptive field centers of the RGCs. Thus, activation of RGCs together with stimulation of the coupled PACs with a contiguous light stimulus was necessary to generate coherent

activity. (K) Cumulative histogram from six pairs of ON α-RGCs shows that the percentage of correlated spike activity did not increase significantly until the rectangles were fused into one single object. One-way ANOVA followed by Tukey's multiple-comparison test at  $\alpha = 0.05$ ; \*\* $P < 0.01$ . Data are presented as mean  $\pm$  SEM.

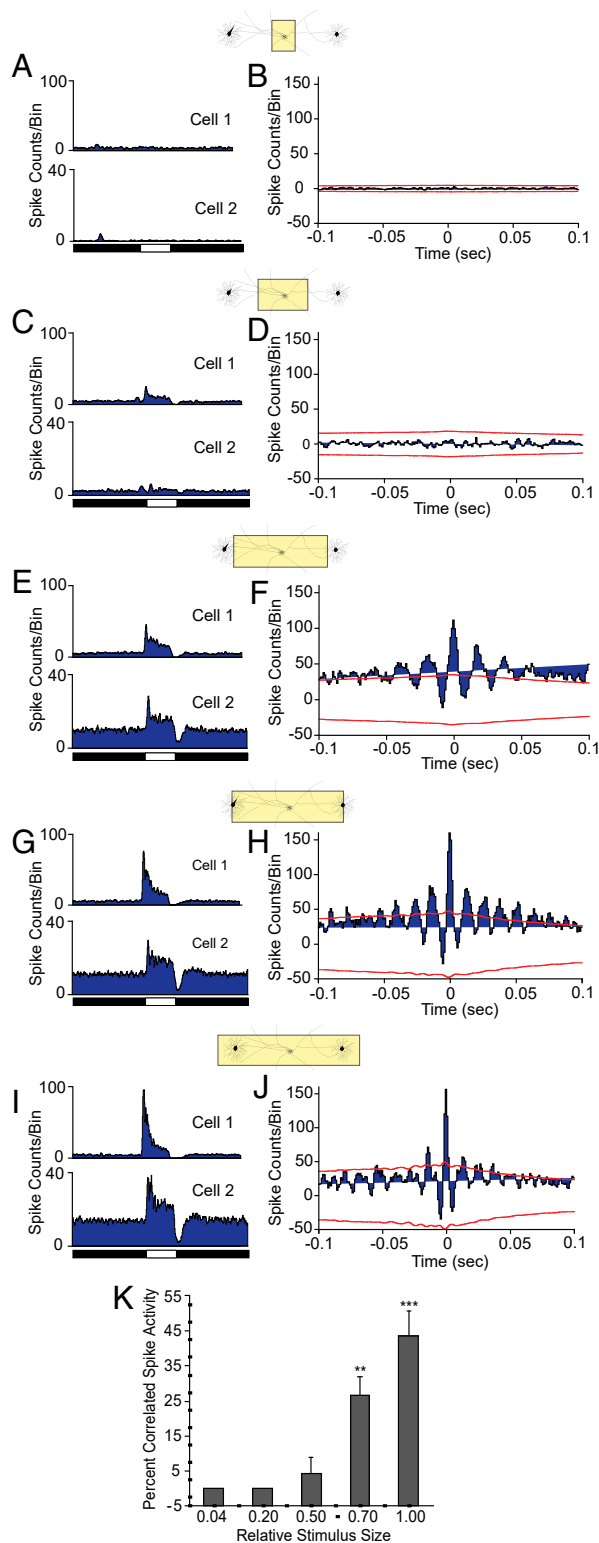


**Fig. 6.** Light stimulation of PACs in the intermediary zone does not evoke long-range coherent activity between ON α-RGC pairs. (A–J) PSTHs (A, C, E, G, and I) and corresponding shift predictor CCPs (B, D, F, H, and J) generated from the light-evoked spike activity recorded from a pair of ON α-RGCs in the Kcng4-YFP mouse retina in response to a single rectangular light stimulus placed between their receptive field centers and increased incrementally (relative size: A and B, 0.04; C and D, 0.20; E and F, 0.50; G and H, 0.70; I and J, 1.00). (K) Cumulative histogram from five ON α-RGC pairs shows a gradual increase of correlated spike activity as the stimulus size is increased, but no significant change until the stimulus covers, at least in part,

RGC firing. One possible scenario, supported by computational modeling, is that RGCs are inhibited by the same PACs that excite them via GJs, and RGC activation is necessary to quash this inhibition, thereby releasing the excitation to produce spike synchrony (51). A similar mechanism is thought to underlie the synchronous activity of pyramidal cells in visual cortex (52).

Interestingly, we found that a small stimulus restricted to the intermediary zone between two widely separated RGCs, believed sufficient to stimulate the coupled PACs, was insufficient to produce coherent RGC activity. Only after the stimulus was enlarged to cover at least part of the RGC receptive field centers was coherent spiking observed. These data suggest that the RGCs must be primed by direct stimulation, likely derived from bipolar cell excitatory inputs, which combines with signals derived from the coupled PACs to produce coherent firing. This notion is consistent with a recent report indicating that coincident electrical and chemical inputs are necessary to produce correlated spiking between RGC neighbors (53). Interestingly, that study also showed that a gap placed within a light stimulus covering the receptive fields of RGC neighbors dramatically reduced spike coherence. Again, the observed loss of spike coherence when a stimulus is disjointed may reflect mediation by an inhibitory mechanism. Clearly, further work is needed to determine the circuitry that produces such fine control of long-range RGC coherent firing.

Utilizing similar paradigms as in the electrophysiological experiments, we found that blockade or ablation of GJs significantly reduced the ability of mice to discriminate large, contiguous objects from disjointed ones. These results support the idea, first suggested by Neuenschwander and Singer (10), that long-range coherent activity between widely separated RGCs encodes information critical to perceptual grouping and global object recognition. Interestingly, as assayed by the level of activity coherence, the RGCs in control retinas reliably responded to stimuli separated by as little as 20 μm, which corresponds to ~0.7° of visual angle in the mouse retina. In contrast, behavioral experiments showed that control mice could not discriminate a solid rectangular stimulus from two rectangles separated by 2° or less. Thus, the RGCs could discriminate discontinuities in objects with better precision than the animals could in perceptual tasks. This difference could reflect technical issues related to (i) potentially superior optics in the *in vitro* experiments in which the anterior optics of the eye were removed and stimuli were projected directly on the retina; and/or (ii) animal performance on the Y water maze task (37). However, we did find that spatial acuity measured from maze behavioral experiments were comparable to values obtained electrophysiologically (54). Alternatively, these data are consistent with the hypothesis that, with the enormous sensory information generated, not all signals reach the brain, but rather bottlenecks are utilized to limit transmission of only the most important details (55).

Natural scenes are inherently complex, and so the visual system must have the capacity to recognize image patterns rapidly and efficiently. It has been advanced that encoding of perceptual objects necessitates the concerted action of large neuronal populations distributed across the visual system (1). Coherent rhythmic brain activity has been studied for over 80 y, and numerous ideas have been forwarded relating to their origin and function (3, 56). In the visual system, beginning in the retina, synchronized activity has been posited to establish relationships among distributed responses, resulting in perceptual grouping critical for distinguishing global objects from the background

the receptive fields of both RGCs. One-way ANOVA followed by Tukey's multiple-comparison test at  $\alpha = 0.05$ ; \*\* $P < 0.01$ ; \*\*\* $P < 0.001$ . Data are presented as mean  $\pm$  SEM.

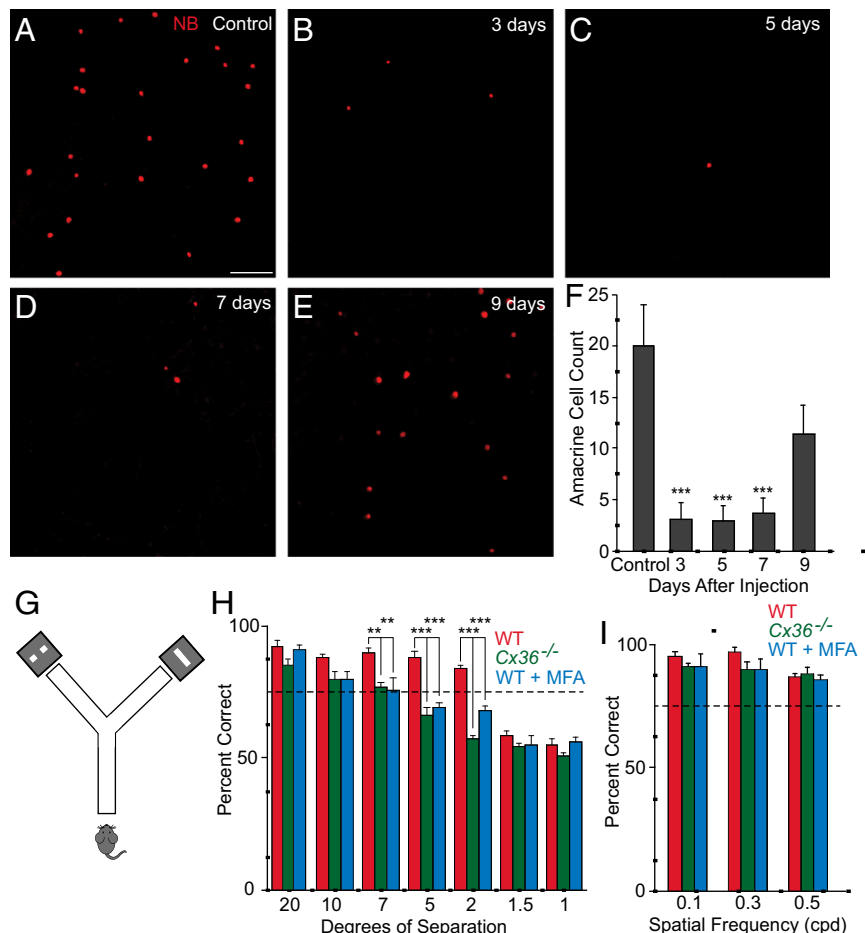


**Fig. 7.** Blockade of retinal GJs or genetic deletion of Cx36 reduces the global object perception of mice compared with their wild-type littermates. (A) Flat-mount view of the proximal inner nuclear layer (INL) shows ACs labeled with NB derived from GJs made with RGCs; RGCs were initially labeled retrogradely by NB injection into the optic nerve. (Scale bar, 100  $\mu$ m.) (B–E) Flat-mount view of the proximal INL at different time points after intravitreal injection of MFA and NB injection into the optic nerve (B, 3 d; C, 5 d; D, 7 d; E, 9 d). Data show that MFA eliminates coupling between RGCs and ACs for up to 7 d after intravitreal injection. (F) Number of ACs labeled with NB at different time points after MFA and NB application. Measures were made within the proximal INL from 600  $\times$  600- $\mu$ m areas in each of four retinal quadrants and averaged ( $n = 3$  retinas). One-way ANOVA with Tukey's multiple-comparison test; \*\*\* $P < 0.001$ . (G) Schematic of the Y water maze used in the behavioral experiments. (H) Cumulative behavioral data from WT and Cx36<sup>-/-</sup> ( $n = 5$  animals for each strain) and WT mice intravitreally injected with MFA (WT + MFA;  $n = 5$  mice for 20°, 5°, 2°;  $n = 3$  mice for 10°, 7°, 1.5°, 1°). The bar graph shows significant attenuation of global object perception in Cx36<sup>-/-</sup> and WT-plus-MFA animals compared with WT mice. Threshold was taken as 75% correct (dashed line). One-way ANOVA with Tukey's multiple-comparison test; \*\* $P < 0.01$ ; \*\*\* $P < 0.001$ . (I) Spatial acuity tested for the same mice as in H using sinusoidal gratings of 0.1, 0.3, and 0.5 cycles per degree (cpd) showed no attenuation in vision between WT, WT-plus-MFA, and Cx36<sup>-/-</sup> mice. One-way ANOVA with Tukey's multiple-comparison test.  $\alpha = 0.05$  for all analyses in the figure. Data presented as mean  $\pm$  SEM.

(56). The present data provide strong evidence that electrical coupling in the retina, specifically between RGCs and PACs, forms the synaptic mechanism responsible for long-range spike synchrony in the retina. In turn, the synchronous activity generated in the retina is believed to be transmitted reliably to the LGN and cortex, suggesting coding essential for perceptual grouping is initialized early in the visual pathways (10). This idea is supported by the results of our behavioral experiments, which showed that long-range coherent activity of RGCs is critical to the perception of global vs. disjointed stimuli. Natural scenes obviously contain far more information than the relatively simple stimuli used in this study, raising the possibility that visual cues in addition to spatial gaps may be utilized for efficient global object perception and perceptual grouping. However, the fact that our simple solid vs. disjointed stimuli were sufficient to reveal differences in electrophysiological and behavioral activity suggests that a very robust mechanism is in place to create the coherent signals critical for global object recognition.

Although our results are consistent with the idea that synchronous activity in retina supports perceptual grouping at the cortical

level, how the cortex decodes this incoming information is unclear. In fact, it has been suggested that, within the primary visual cortex, perceptual grouping is achieved by enhancement of the mean firing rate of neurons rather than synchrony (21, 57). Likewise, psychophysical experiments suggest that coherent activity, at least at the cortical level, is not responsible for perceptual grouping (58). While these data would appear to conflict with the present findings, it is important to emphasize that the mechanism by which the retina encodes visual information may be dissimilar to the mechanism by which it is decoded in the cortex. Thus, whereas our results indicate that synchronous spikes generated in retina provide information to central targets critical to global object recognition, the decoding process may give rise to an alternate neural code at the cortical level with different temporal and rate properties (59).

## Methods

Electrophysiological and behavioral experiments were conducted on retinas from wild-type C57BL/6, transgenic Kcng4-YFP, Cx36<sup>-/-</sup>, and their wild-type littermate (CxWT) mouse strains. Pairwise loose-patch recordings were made from  $\alpha$ -RGCs that were widely separated by 300–600  $\mu$ m, corresponding to

~12–24° of visual angle. The α-RGCs were categorized as ON or OFF based on their response to stimulus onset or offset. Moreover, we found that the ON α-RGC showed sustained responses, whereas the OFF α-RGC showed transient or sustained responses, confirming previous reports (60, 61). Recordings were made from pairs of transient OFF α-RGCs or pairs of sustained OFF α-RGCs. Concerted spike activity was computed between RGCs by creating CCPs under control conditions or after retina GJs were blocked pharmacologically by application of MFA. Parallel experiments were carried out on Cx36<sup>-/-</sup> and CxWT mice. For behavioral experiments, animals were trained on a Y water maze to discriminate between a solid, contiguous object and a disjointed as well as spatial sinusoidal grating to test spatial acuity. Com-

parisons were made between control wild-type mice and those receiving bilateral intravitreal injections of MFA as well as between CxWT and Cx36<sup>-/-</sup> mice. For methodological details, see *Supporting Information*.

All animal procedures were carried out in compliance with the National Institutes of Health Guide for Care and Use of Laboratory Animals (62) and approved by the Institutional Animal Care and Use Committee at the State University of New York, College of Optometry.

**ACKNOWLEDGMENTS.** We thank Dr. Joshua Sanes for providing the Kcng4-cre and Thy1-line 1 transgenic mouse strains. This work was supported by NIH Grant EY007360.

1. Singer W, Gray CM (1995) Visual feature integration and the temporal correlation hypothesis. *Annu Rev Neurosci* 18:555–586.
2. Singer W (1999) Neuronal synchrony: A versatile code for the definition of relations? *Neuron* 24:49–65, 111–125.
3. Steriade M (2006) Grouping of brain rhythms in corticothalamic systems. *Neuroscience* 137:1087–1106.
4. Mastronarde DN (1983) Interactions between ganglion cells in cat retina. *J Neurophysiol* 49:350–365.
5. Mastronarde DN (1983) Correlated firing of cat retinal ganglion cells. II. Responses of X and Y-cells to single quantal events. *J Neurophysiol* 49:325–349.
6. Mastronarde DN (1983) Correlated firing of cat retinal ganglion cells. I. Spontaneously active inputs to X- and Y-cells. *J Neurophysiol* 49:303–324.
7. Meister M, Lagnado L, Baylor DA (1995) Concerted signaling by retinal ganglion cells. *Science* 270:1207–1210.
8. Brivanlou IH, Warland DK, Meister M (1998) Mechanisms of concerted firing among retinal ganglion cells. *Neuron* 20:527–539.
9. DeVries SH (1999) Correlated firing in rabbit retinal ganglion cells. *J Neurophysiol* 81:908–920.
10. Neuenschwander S, Singer W (1996) Long-range synchronization of oscillatory light responses in the cat retina and lateral geniculate nucleus. *Nature* 379:728–732.
11. Ishikane H, Kawana A, Tachibana M (1999) Short- and long-range synchronous activities in dimming detectors of the frog retina. *Vis Neurosci* 16:1001–1014.
12. Hu EH, Pan F, Völgyi B, Bloomfield SA (2010) Light increases the gap junctional coupling of retinal ganglion cells. *J Physiol* 588:4145–4163.
13. Meister M, Berry MJ, 2nd (1999) The neural code of the retina. *Neuron* 22:435–450.
14. Pillow JW, et al. (2008) Spatio-temporal correlations and visual signalling in a complete neuronal population. *Nature* 454:995–999.
15. Shadlen MN, Newsome WT (1998) The variable discharge of cortical neurons: Implications for connectivity, computation, and information coding. *J Neurosci* 18:3870–3896.
16. Nirenberg S, Carcieri SM, Jacobs AL, Latham PE (2001) Retinal ganglion cells act largely as independent encoders. *Nature* 411:698–701.
17. Mazurek ME, Shadlen MN (2002) Limits to the temporal fidelity of cortical spike rate signals. *Nat Neurosci* 5:463–471.
18. Puchalla JL, Schneidman E, Harris RA, Berry MJ (2005) Redundancy in the population code of the retina. *Neuron* 46:493–504.
19. Roelfsema PR, Singer W (1998) Detecting connectedness. *Cereb Cortex* 8:385–396.
20. Shadlen MN, Movshon JA (1999) Synchrony unbound: A critical evaluation of the temporal binding hypothesis. *Neuron* 24:67–77, 111–125.
21. Roelfsema PR, Lamme VA, Spekreijse H (2004) Synchrony and covariation of firing rates in the primary visual cortex during contour grouping. *Nat Neurosci* 7:982–991.
22. Söhl G, Maxeiner S, Willecke K (2005) Expression and functions of neuronal gap junctions. *Nat Rev Neurosci* 6:191–200.
23. Meier C, Dermietzel R (2006) Electrical synapses—gap junctions in the brain. *Results Probl Cell Differ* 43:99–128.
24. Bloomfield SA, Völgyi B (2009) The diverse functional roles and regulation of neuronal gap junctions in the retina. *Nat Rev Neurosci* 10:495–506.
25. Völgyi B, Xin D, Amarillo Y, Bloomfield SA (2001) Morphology and physiology of the polyaxonal amacrine cells in the rabbit retina. *J Comp Neurol* 440:109–125.
26. Völgyi B, Chheda S, Bloomfield SA (2009) Tracer coupling patterns of the ganglion cell subtypes in the mouse retina. *J Comp Neurol* 512:664–687.
27. Xin D, Bloomfield SA (1997) Tracer coupling pattern of amacrine and ganglion cells in the rabbit retina. *J Comp Neurol* 383:512–528.
28. Duan X, Krishnaswamy A, De la Huerta I, Sanes JR (2014) Type II cadherins guide assembly of a direction-selective retinal circuit. *Cell* 158:793–807.
29. Duan X, et al. (2015) Subtype-specific regeneration of retinal ganglion cells following axotomy: Effects of osteopontin and mTOR signaling. *Neuron* 85:1244–1256.
30. Meller D, Eysel UT, Schmidt-Kastner R (1994) Transient immunohistochemical labelling of rat retinal axons during wallerian degeneration by a monoclonal antibody to neurofilaments. *Brain Res* 648:162–166.
31. Perkel DH, Gerstein GL, Moore GP (1967) Neuronal spike trains and stochastic point processes. II. Simultaneous spike trains. *Biophys J* 7:419–440.
32. Völgyi B, et al. (2013) Gap junctions are essential for generating the correlated spike activity of neighboring retinal ganglion cells. *PLoS One* 8:e69426.
33. Pan F, Paul DL, Bloomfield SA, Völgyi B (2010) Connexin36 is required for gap junctional coupling of most ganglion cell subtypes in the mouse retina. *J Comp Neurol* 518:911–927.
34. Völgyi B, Abrams J, Paul DL, Bloomfield SA (2005) Morphology and tracer coupling pattern of alpha ganglion cells in the mouse retina. *J Comp Neurol* 492:66–77.
35. Davenport CM, Detwiler PB, Dacey DM (2007) Functional polarity of dendrites and axons of primate A1 amacrine cells. *Vis Neurosci* 24:449–457.
36. Greschner M, et al. (2014) A polyaxonal amacrine cell population in the primate retina. *J Neurosci* 34:3597–3606.
37. Prusky GT, West PW, Douglas RM (2000) Behavioral assessment of visual acuity in mice and rats. *Vision Res* 40:2201–2209.
38. Stafford DK, Dacey DM (1997) Physiology of the A1 amacrine: A spiking, axon-bearing interneuron of the macaque monkey retina. *Vis Neurosci* 14:507–522.
39. Wright LL, Vaney DI (2004) The type 1 polyaxonal amacrine cells of the rabbit retina: A tracer-coupling study. *Vis Neurosci* 21:145–155.
40. Kalloniatis M, Marc RE, Murry RF (1996) Amino acid signatures in the primate retina. *J Neurosci* 16:6807–6829.
41. Marc RE, Jones BW (2002) Molecular phenotyping of retinal ganglion cells. *J Neurosci* 22:413–427.
42. Wässle H, Grünert U, Röhrenbeck J, Boycott BB (1990) Retinal ganglion cell density and cortical magnification factor in the primate. *Vision Res* 30:1897–1911.
43. Pang JJ, Paul DL, Wu SM (2013) Survey on amacrine cells coupling to retrogradely identified ganglion cells in the mouse retina. *Invest Ophthalmol Vis Sci* 54:5151–5162.
44. Demb JB, Haarsma L, Freed MA, Sterling P (1999) Functional circuitry of the retinal ganglion cell's nonlinear receptive field. *J Neurosci* 19:9756–9767.
45. Derrington AM, Lennie P, Wright MJ (1979) The mechanism of peripherally evoked responses in retinal ganglion cells. *J Physiol* 289:299–310.
46. McIlwain JT (1964) Receptive fields of optic tract axons and lateral geniculate cells: Peripheral extent and barbiturate sensitivity. *J Neurophysiol* 27:1154–1173.
47. Kenyon GT, et al. (2003) A model of high-frequency oscillatory potentials in retinal ganglion cells. *Vis Neurosci* 20:465–480.
48. Hu EH, Bloomfield SA (2003) Gap junctional coupling underlies the short-latency spike synchrony of retinal alpha ganglion cells. *J Neurosci* 23:6768–6777.
49. Kenyon GT, et al. (2004) Stimulus-specific oscillations in a retinal model. *IEEE Trans Neural Netw* 15:1083–1091.
50. Ackert JM, Farajian R, Völgyi B, Bloomfield SA (2009) GABA blockade unmasks an OFF response in ON direction selective ganglion cells in the mammalian retina. *J Physiol* 587:4481–4495.
51. Kenyon GT, Marshak DW (1998) Gap junctions with amacrine cells provide a feedback pathway for ganglion cells within the retina. *Proc Biol Sci* 265:919–925.
52. Bush P, Sejnowski T (1996) Inhibition synchronizes sparsely connected cortical neurons within and between columns in realistic network models. *J Comput Neurosci* 3:91–110.
53. Trenholm S, et al. (2014) Nonlinear dendritic integration of electrical and chemical synaptic inputs drives fine-scale correlations. *Nat Neurosci* 17:1759–1766.
54. Porciatti V, Pizzorusso T, Maffei L (1999) The visual physiology of the wild type mouse determined with pattern VEPs. *Vision Res* 39:3071–3081.
55. Gray CM (1999) The temporal correlation hypothesis of visual feature integration: Still alive and well. *Neuron* 24:31–47, 111–125.
56. Singer W, et al. (1997) Neuronal assemblies: Necessity, signature and detectability. *Trends Cogn Sci* 1:252–261.
57. Gilad A, Slovin H (2015) Population responses in V1 encode different figures by response amplitude. *J Neurosci* 35:6335–6349.
58. Kiper DC, Gegenfurtner KR, Movshon JA (1996) Cortical oscillatory responses do not affect visual segmentation. *Vision Res* 36:539–544.
59. Ainsworth M, et al. (2012) Rates and rhythms: A synergistic view of frequency and temporal coding in neuronal networks. *Neuron* 75:572–583.
60. Pang JJ, Gao F, Wu SM (2003) Light-evoked excitatory and inhibitory synaptic inputs to ON and OFF alpha ganglion cells in the mouse retina. *J Neurosci* 23:6063–6073.
61. van Wyk M, Wässle H, Taylor WR (2009) Receptive field properties of ON- and OFF-ganglion cells in the mouse retina. *Vis Neurosci* 26:297–308.
62. National Research Council (2011) *Guide for the Care and Use of Laboratory Animals* (National Academies Press, Washington, DC), 8th Ed.
63. Deans MR, Gibson JR, Sellitto C, Connors BW, Paul DL (2001) Synchronous activity of inhibitory networks in neocortex requires electrical synapses containing connexin36. *Neuron* 31:477–485.
64. Deans MR, Völgyi B, Goodenough DA, Bloomfield SA, Paul DL (2002) Connexin36 is essential for transmission of rod-mediated visual signals in the mammalian retina. *Neuron* 36:703–712.
65. Akopian A, et al. (2014) Gap junction-mediated death of retinal neurons is connexin and insult specific: A potential target for neuroprotection. *J Neurosci* 34:10582–10591.
66. Brainard DH (1997) The Psychophysics Toolbox. *Spat Vis* 10:433–436.
67. Gellermann LW (1933) Chance orders of alternating stimuli in visual discrimination experiments. *J Genet Psychol* 42:206–208.